INSTITUTE OF PHYSICS PUBLISHING PLASMA PHYSICS AND CONTROLLED FUSION

Plasma Phys. Control. Fusion **47** (2005) B859–B867 doi:10.1088/0741-3335/47/12B/S68

Direct-drive fuel-assembly experiments with gas-filled, cone-in-shell, fast-ignitor targets on the OMEGA Laser

C Stoeckl[1], T R Boehly[1], J A Delettrez[1], S P Hatchett[2], J A Frenje[3], V Yu Glebov[1], C K Li[3], J E Miller[1], R D Petrasso[3], F H Séguin[3], V A Smalyuk[1], R B Stephens[4], W Theobald[1], B Yaakobi[1] and T C Sangster[1]

[1] Laboratory for Laser Energetics, University of Rochester, Rochester, NY, USA
[2] Lawrence Livermore National Laboratory, Livermore, CA, USA
[3] Plasma Science and Fusion Center, Massachusetts Institute of Technology, Cambridge, MA, USA
[4] General Atomics, San Diego, CA, USA

Received 1 July 2005
Published 14 November 2005
Online at stacks.iop.org/PPCF/47/B859

Abstract

The fuel assembly of gas-filled, cone-in-shell, fast-ignitor targets is being studied experimentally at the OMEGA Laser Facility. The spherical plastic (CH) shells with a $\sim$24 μm wall thickness had a 70° or 35° opening-angle gold cone inserted. The targets, filled with $\sim$10 atm of D^3He or D_2, were imploded by direct illumination with up to 21 kJ of 351 nm laser light. Some experiments used a backlighter to study the fuel assembly and mixing of cone material into the dense core. No significant mixing of the cone and core material was observed. Using both fusion products and backlit images, an areal density of $\sim$60 to 70 mg cm^{-2} was inferred for the dense core assembly. The filling of the inside of the cone, where the ultrafast laser propagates in integrated fast-ignitor experiments, was studied using a streaked optical pyrometer. No plasma was seen inside the cone before the assembled core reached peak compression. These results are promising for successful integrated fast-ignitor experiments on the OMEGA EP Facility, scheduled to be completed in 2007.

1. Introduction

The fast-ignitor concept for inertial confinement fusion [1, 2] has the potential for higher gains and lower driver energies than conventional spark ignition [3]. The fast-ignitor concept separates the fuel assembly and heating by using an ultrafast laser. The ultrafast laser produces relativistic electrons with high efficiency (up to 50% has been reported [4]) that heat the fuel, significantly easing the requirements on the compression driver [2, 5]. Laser or heavy-ion beam heated hohlraums and direct-drive laser are options for the compression driver.

The biggest challenge of the fast-ignitor concept is the transport of the relativistic electrons from the critical-density region ($n_e \sim 10^{21}$ cm^{-3} for a typical 1 μm laser), where the ultrafast laser is absorbed and converted into electrons, to the compressed fuel—a distance that can be hundreds of micrometres in an ignition-scale target. For an electron beam divergence of >20°, the overlap between the electron beam originating from a small focal spot (~10 μm radius) and the dense core with a diameter of <50 μm would be very small [6, 7]. Most of the energy in the electron beam would be wasted. Two solutions have been proposed to minimize this standoff distance: a channelling beam to bore a hole in the plasma atmosphere around the core [2, 8] that allows the ultrafast laser to be absorbed closer to the core and a re-entrant cone to keep the path of the ultrafast laser free of plasma and bring it as close as possible to the dense core [9–11].

A few experiments have been performed to assess the potential of the re-entrant cone concept. Integrated experiments at ILE, Osaka examined the coupling between the electron beam and the compressed core and found a 20–30% energy transfer [11, 12], and a 1000-fold increase in neutron yield from 10^4 to 10^7 was observed by coupling a 0.5 PW, short-pulse laser into an empty CD target imploded by 2.5 kJ of laser light at a wavelength of 0.53 μm. A first series of hydroflow experiments [13] with re-entrant cone targets in an indirect-drive geometry on OMEGA was conducted to study the fuel assembly with 1 kJ of x-ray energy coupled to the capsule. Significant mixing between the gold cone and the plastic shell material was observed. Mixing gold into the dense fuel/shell material substantially increases the required ignition energy. Stephens *et al* [13] predicted that using direct drive would minimize the mixing between the gold cone and the fuel/shell material. Another issue for cone targets is plasma filling the inside of the cone, where the ultrafast laser has to propagate. The high-pressure core plasma sends a shock wave through the gold cone that creates a plasma inside the cone when it breaks out, significantly increasing the electron propagation distance.

Fuel-assembly experiments with gas-filled, direct-drive, re-entrant cone-in-shell targets were performed on the OMEGA Laser System [14] to study whether the cone-in-shell design is scalable to higher-energy densities and in preparation for future integrated experiments on the OMEGA EP laser [15, 16] which will be operational in 2007. The experimental set-up is described in section 2, including the laser configuration and imaging diagnostic arrangement. Section 3 discusses the backlighting of the fuel assembly of 70° and 35° cone targets. Section 4 analyses the mixing of the cone and shell material and section 5 describes areal-density measurements carried out using nuclear diagnostic methods. Section 6 deals with measurements of the shock breakout into the inside of the cone. Section 7 describes prospects for integrated experiments using the OMEGA EP laser and concludes.

2. Experimental set-up

Several different laser configurations were used for the direct-drive, cone-in-shell experiments on the 60 beam OMEGA laser. The targets were illuminated at a wavelength of 351 nm with a 1 ns square pulse and an energy of 400 J per beam using two-dimensional smoothing by spectral dispersion (SSD) [17] with 1 THz bandwidth in the UV and polarization smoothing (PS) [18]. The beams driving the shell used distributed phase plates (DPPs) [19]. For the backlighting experiments, 15 beams (~6 kJ energy) were diverted to a backlighter foil of either vanadium (V) or iron (Fe) and focused to a spot size of 600 μm without DPPs. To provide a nearly uniform illumination of the shell, 15 beams were run at half energy and 20 beams at full energy, a total of ~11 kJ of laser energy driving the implosion. The nuclear diagnostics experiments used 55 beams, with ~21 kJ of total energy. The cone-filling experiments used 48 beams for

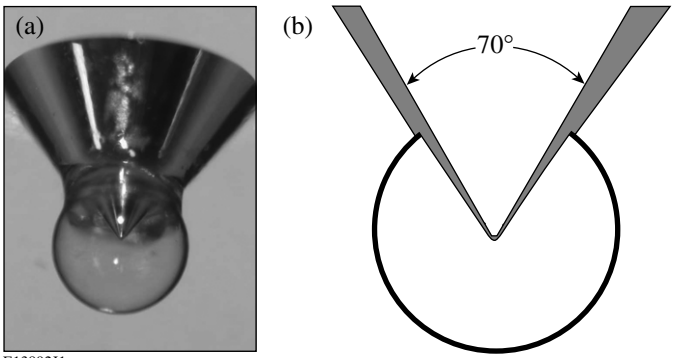

Figure 1. Picture of a gas-tight, fast-ignitor cone target (*a*) and a schematic of its cross section (*b*). A gold cone with an opening angle of 70° is inserted through a hole in a 24 μm thick CH shell of ~870 μm outer diameter.

the 70° cones or 54 beams for the 35° cones to avoid the laser hitting the inside of the cones. A small amount of direct and reflected laser light hit the outside of the cone in all experiments.

The targets consist of gas-tight, ~870 μm outer-diameter, 24 μm thick CH shells with a hollow gold cone with an opening angle of 70° or 35° inserted through a hole in the shell (see figure 1). The distance between the cone tip and the centre of the shell, typically 30 ± 10 μm, is defined by a shelf on the cone that provides a gas-tight interface for the assembly. Both the 70° and 35° gold cones had a thickness of ~100 μm outside the shell, ~10 μm inside the shell, and ended in a hyperbolic-shaped tip with the asymptotes intersecting 12 μm from the target centre, resulting in an Au thickness of ~30 μm at the tip of the cone. Time-resolved x-ray framing cameras [20] recorded both backlit and self-emission images. The backlighter framing camera had an exposure time of ~40 ps, and the self-emission camera, ~80 ps. The framing cameras acquired 16 images with a ~60 ps temporal separation between exposures. Both cameras used a pinhole imager with a spatial resolution of ~10 μm in the target plane. The self-emission camera was filtered with ~200 μm of Be, with a lower cutoff at 50% transmission of ~3 keV. The backlighter camera used either a 25 μm thick V filter to pass the predominantly He_α line emission of the V backlighter at 4.95 keV or a 25 μm thick Fe filter for the He_α line emission of a Fe backlighter at 6.7 keV. These filters suppress the thermal radiation from the implosion, improving the contrast of the backlit images.

3. Fuel assembly in 70° and 35° cone targets

A comparison of the fuel assembly of the 35° and 70° cone targets is shown in figure 2. Backlit images from unfilled 35° (figure 2(*a*)) and 70° (figure 2(*b*)) targets were recorded using a Fe backlighter. Three images spaced ~250 ps apart show the assembly of the core, with the central image close to the time of peak compression. The core assembly is similar in the two cases, particularly the evolution of the core size. At early times, a horseshoe-shaped dense area is observed, with the opening towards the cone as expected. At peak compression, the core looks quite round and symmetric, with no influence of the cone visible. At this time the distance from the tip of the cone to the core is of the order of 50 μm in both cases. After peak compression, the core expands in an almost symmetric fashion. Both targets exhaust plasma towards the tip of the cone, eroding the tip of the cone at later times. The 35° targets shows less backlighter absorption in the core than do the 70° cone targets, possibly due to the incomplete suppression

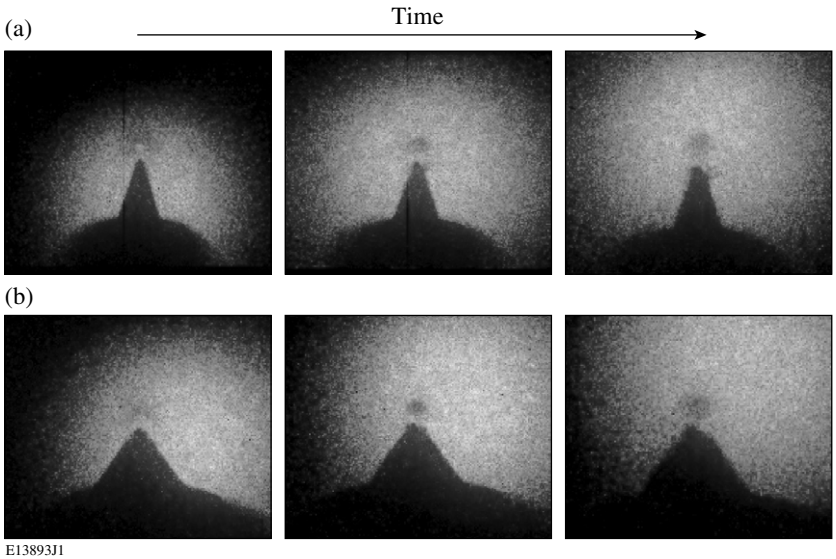

Figure 2. Backlit framing camera images from a 35° cone target (*a*) and 70° target (*b*) obtained using a Fe backlighter. Three images spaced ∼250 ps apart show the assembly of the core and the erosion of the cone, with the central image close to the time of peak compression.

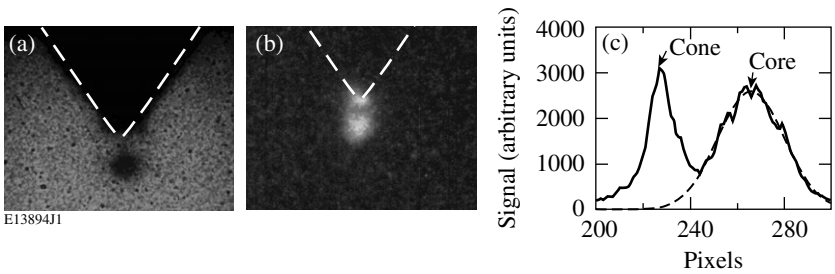

Figure 3. (*a*) Backlit and (*b*) self-emission x-ray framing camera images of unfilled cone targets obtained using pinhole imaging taken at peak compression. The extent of the cone before the laser shot is indicated with dashed lines. A lineout through the self-emission image is shown in (*c*).

of the core self-emission, since the narrow cones are expected to disturb the implosion less and lead to higher core temperatures. The images also show that the plasma flow is directed from the core towards the tip of the cone, an indication that the mixing of gold and the core material is not significant in these implosions.

4. Mixing of Au cone and core material

Unfilled capsules were used to evaluate the mixing of the gold cone with the CH shell material to compare with previous indirect-drive experiments [13]. Figure 3 shows a backlit (*a*) image obtained using a V backlighter and a self-emission (*b*) image taken at the time of peak compression. The backlit image shows absorption outside the original extent of the cone as indicated by the dashed lines, showing that an expanding plasma is created on the surface of the cone. A gap between the cone tip and core assembly is seen in both images, unlike in

the data obtained using indirect drive [13]. The indirect-drive data were interpreted as a 0.04% mass density gold contamination in the compressed shell material. No mixing is seen in direct drive, which can be attributed in part to less material ablated from the gold cone in direct drive as predicted in [13]. A change in the target design, the introduction of a shelf, where the cone rests on the shell (see figure 1(*b*)), keeping the incoming shell material away from the cone, could have helped to reduce mixing. There is no indication that the laser light hitting the gold cone on the outside affects the mixing significantly. An estimate of the minimum detectable gold contamination can be obtained from analysis of the self-emission images. Figure 3(*c*) shows a lineout through the centre of the self-emission image. A Gaussian fit to the core emission shows that there is no indication of extra emission on the left side towards the cone due to Au mixing into the core. At high temperatures (>1 keV) and moderate densities (<1 g cm^{-3}), the plasma conditions expected in the gap, the CH emissivity at 2–3 keV is roughly 2000 times smaller than the Au opacity. Consequently, a gold contamination of the order of 0.01% of the mass density in the gap would be visible as a ∼10% enhancement of the emission, the estimated error of the symmetry of the emission profile. X-ray emission from shell plasma in the gap between the cone and core reduces the absorption minimum seen in the backlit image. This can be corrected using the self-emission images that show that the emission intensity in the gap is about $\frac{1}{3}$ of the emission at the centre of the collapsed shell. An analysis of corrected backlit images analogous to that of the self-emission images using the cold Au and the hot CH opacities shows no indication of gold plasma streaming into the core with a detection threshold of roughly 0.01% of the mass density.

5. Compressed core areal density measurements

The areal density of the assembled core was determined from experiments with targets filled with D^3He gas using nuclear diagnostics. Because of the strong He x-ray emission, the size and location of the hot-fuel region can be inferred from x-ray images of D^3He-filled targets. Figure 4(*a*) shows a backlit x-ray image of a 70° cone target filled with 10 atm, D^3He obtained at the time of peak proton production using a Fe backlighter at 6.7 keV. Wedged-range-filter spectrometers [21] are used to infer the areal density of the compressed shell [22, 23] from the energy loss of the 14.7 MeV primary fusion protons. The proton spectrometers are deployed in two different directions ∼15 cm from the target. Figure 4(*a*) shows the line of sight of the two proton spectrometers (labelled TIM1 and TIM3). Figure 4 also shows the proton spectra from three 35° cone targets imploded with 55 beams at 21 kJ with a total a proton yield (∼3×10^6) integrated onto the wedged-range filters in TIM3 (*b*) and TIM1 (*c*). Two peaks are observed in the TIM3 spectrum because the protons detected in TIM3 pass through the dense core (see figure 4). The narrow peak at ∼14 MeV is attributed to the shock coalescence phase of the implosion, when the assembled areal density is low [23]. The second broader peak at ∼12 MeV is due to protons passing through the dense core close to peak compression [23]. An areal density of ∼70 ± 5 mg cm^{-2} is inferred from the average-energy downshift of ∼2 MeV [21]. The protons detected at TIM2 from both the shock and compression phase experience little energy loss and produce only a single narrow peak. The proton yields from the 70° cone targets were about a factor of 2 lower than the yields recorded from the 35° cone targets and showed marginally lower areal densities of ∼60 ± 10 mg cm^{-2}. A rough estimate of the core average mass density of ∼10 g cm^{-3} can be obtained from the areal densities by using the radius of the compressed core from figure 2 of ∼60 μm. A fuel ion temperature of 1.2 ± 0.4 keV was inferred from the ratio of the D^3He proton and the DD neutron yields [22].

The experimental areal density values were compared to simulations of full-sphere (no cone) implosions using the 1-D hydrocode LILAC [24]. LILAC predicts a total areal

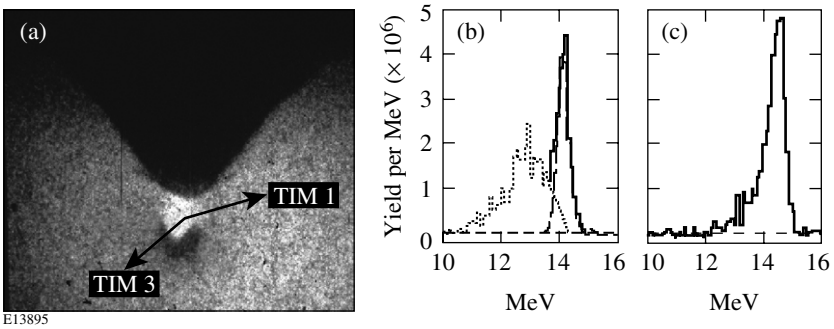

Figure 4. Backlit image (*a*) of a 10 atm, D^3He-filled cone target at the time of peak proton production obtained using a Fe backlighter. Significant self-emission from the hot D^3He gas is seen in the image. The directions of the proton spectrometers used to determine the core areal density are indicated as TIM1 and TIM3. D^3He proton spectra taken along two different lines of sight: TIM3 (*b*) and TIM1 (*c*).

density (shell and fuel) of $\sim$90 mg cm^{-2} at the time of peak proton emission for a 24 μm thick full spherical shell with an average ion temperature of 2.3 keV and a total proton yield of 3×10^8.

The average mass density at peak proton emission is $\sim$15 g cm^{-3}. The experimental areal density values are more than 66% of the predicted values in both cases, indicating that the presence of the cone does not significantly disturb the fuel assembly. The measured ion temperature is a factor of 2 lower, and the measured proton yield is almost three orders of magnitude lower than the simulation yield, showing that the presence of the cone reduces the central hot-spot temperature. Breaking the spherical symmetry by introducing a cone in the shell affects the ion temperature and consequently the proton yield much more than the fuel assembly and the core areal density. An areal density higher than that of the 1-D predictions due to the lower backpressure from the low-temperature hot spot is not seen; the missing inflow from the cone region seems to be the dominant mechanism in determining the observed areal density. Reducing the cone angle from 70° to 35° has a small effect on the areal density. It improves the yield by a factor of 2, though it is still very far from the 1-D predictions.

6. Cone filling

The filling of the inside of the cones was investigated using a streaked optical pyrometer (SOP) [25] (see figure 5). The SOP optical system images the inside of the tip of the cone onto the slit of the streak camera with a $\sim$10 μm spatial resolution and a 500 μm field of view. The camera is filtered to record in a wavelength band centred at 660 nm with a 140 nm FWHM to minimize the background from scattered 3ω, 2ω and 1ω laser light. The breakout of the shock produces a short burst of light. Its timing relative to the peak compression can be determined from the absolute temporal calibration of the SOP with an uncertainty of 50 ps. The shock temperature is inferred from the observed light signal using the absolute calibration of the SOP in intensity with an uncertainty of 10% above $\sim$1 eV [26]. The number of laser beams used to drive the target is limited to prevent laser light from hitting the inside of the cone and produce a high background signal on the SOP. Figure 6(*a*) shows the SOP streak signal from a 70° cone target irradiated by 48 OMEGA beams with a total energy of $\sim$18 kJ in a 1 ns square pulse. The time axis zero represents the start of the laser pulse. A very clean shock-breakout signal can be seen starting at the tip of the cone and becoming less intense and moving away from the tip as time progresses. Figure 6(*b*) shows a lineout through the

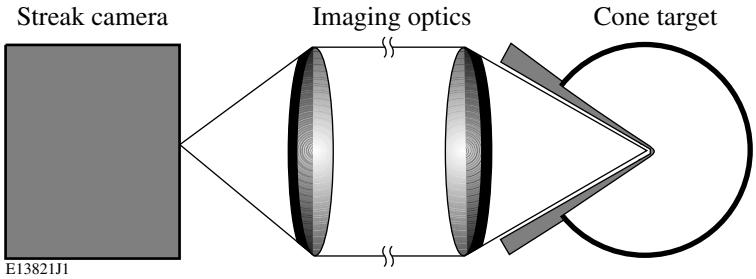

Figure 5. SOP set-up used to investigate the filling of the inside of the cone.

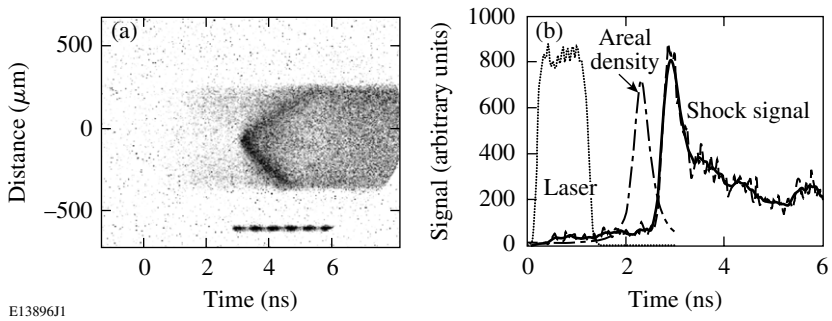

Figure 6. Streaked SOP signal from a 70° cone target (*a*) showing a clean shock breakout. A lineout through the centre of the SOP signal (thick solid line) is shown in (*b*). The thin solid line shows the laser pulse power and the dashed line represents the calculated evolution of the areal density.

centre of the SOP trace in comparison with 1-D hydrocode simulations from LILAC of the total areal density of the compressed core for a spherical target. The 70° cone targets show a clean shock-breakout signal, as in data obtained from planar shock experiments [27]. The shock signal starts well after the time of peak compression (∼500 ps) as calculated by LILAC, showing that the inside of the cone is free of plasma at the time when the short-pulse laser would propagate. An estimated shock temperature of ∼10 eV is obtained using the absolute intensity calibration of SOP.

7. Conclusions and outlook for OMEGA EP

Fuel-assembly experiments with laser-irradiated, cone-in-shell targets performed on OMEGA indicate that this fast-ignition concept is likely to be scalable to higher energy cryogenic targets. No significant mixing of the gold from the cone with the fuel/shell material was observed, in contrast to earlier results of indirect-drive experiments. The core assembly is not severely affected by the presence of the cone, and more than 66% of the expected areal density is inferred from the experiments. Shock-breakout plasma does not begin filling the inside of the cone before peak compression when the ultrafast laser propagates.

In a cryogenic DT ignition capsule, the final core density will be higher, but the core pressure will be similar due to the lower average ionization of the DT compared to CH and the lower adiabat drive [28]. This limits the strength and speed of the shock that causes the inside of the cone to fill with plasma and the erosion of the cone by the core plasma. The thin (1–5 μm) plastic shell containing the cryogenic fuel radiates much less in cryogenic implosions, reducing

the heating and expansion of the gold cone at early times, which minimizes the amount of Au that can mix with the fuel.

Integrated fast-ignitor experiments will be performed at the OMEGA facility using the OMEGA EP Laser System, with its unique capability to compress cryogenic D_2 and DT targets [28, 29]. OMEGA EP will have two short-pulse (∼1–100 ps), high-energy laser beams with up to 2.6 kJ per beam at 1.053 μm. The beams will be combined collinearly and coaxially and routed into the existing OMEGA target chamber. Both integrated cryogenic channelling and re-entrant cone fast-ignitor experiments will be performed. The OMEGA EP laser pulse will be focused to a $\leqslant 10\,\mu$m radius spot with an $f/2$ off-axis parabola, synchronized to the OMEGA laser to better than 10 ps rms, and will be pointed to better than 10 μm accuracy to provide good spatial and temporal overlap between the electron beam and the dense core. Simulations, including alpha transport, of an OMEGA cryogenic target designed to reach a 1-D fuel ρR of 500 mg cm^{-2} have been carried out showing a factor of 10 increase in neutron yield from 10^{14} to 10^{15} and early signatures of alpha heating [30]. Of all laser facilities worldwide, the combined OMEGA/OMEGA EP will be the best suited to perform the next-generation integrated fast-ignition experiments beginning in 2008, significantly advancing our understanding of the fast-ignitor concept.

Acknowledgments

The authors are indebted to the Target Fabrication Groups at GA and LLE, especially Mark Bonino, Abbas Nikroo and Joe Smith. This work was supported by the U.S. Department of Energy Office of Inertial Confinement Fusion under Cooperative Agreement No DE-FC52-92SF19460, the University of Rochester and the New York State Energy Research and Development Authority, with corporate support from General Atomics. The support of DOE does not constitute an endorsement by DOE of the views expressed in this paper.

References

[1] Basov N G, Gus'kov S Y and Feokistov L P 1992 *J. Sov. Laser Res.* **13** 396
[2] Tabak M *et al* 1994 *Phys. Plasmas* **1** 1626
[3] Lindl J D, McCrory R L and Campbell E M 1992 *Phys. Today* **45** 32
[4] Yasuike K *et al* 2001 *Rev. Sci. Instrum.* **72** 1236
[5] Atzeni S 1999 *Phys. Plasmas* **6** 3316
[6] Li Y T *et al* 2004 *Phys. Rev.* E **69** 036405
[7] Stephens R B *et al* 2004 *Phys. Rev.* E **69** 066414
[8] Kitagawa Y *et al* 2002 *Phys. Plasmas* **9** 2202
[9] Tabak M *et al* 1997 *Lawrence Livermore National Laboratory Patent Disclosure* IL-8826B, Lawrence Livermore National Laboratory, Livermore, CA
[10] Norreys P A *et al* 2000 *Phys. Plasmas* **7** 3721
[11] Kodama R *et al* 2001 *Nature* **412** 798
[12] Kodama R *et al* 2002 *Nature* **418** 933
[13] Stephens R B *et al* 2003 *Phys. Rev. Lett.* **91** 185001
[14] Boehly T R *et al* 1997 *Opt. Commun.* **133** 495
[15] Stoeckl C *et al* High-energy petawatt project at the University of Rochester's Laboratory for Laser Energetics *Fusion Sci. Technol.* at press
[16] Waxer L J *et al* 2005 *Opt. Photon. News* July/August 31
[17] Skupsky S and Craxton R S 1999 *Phys. Plasmas* **6** 2157
[18] Boehly T R *et al* 1999 *J. Appl. Phys.* **85** 3444
[19] Lin Y, Kessler T J and Lawrence G N 1996 *Opt. Lett.* **21** 1703
[20] Bradley D K *et al* 1995 *Rev. Sci. Instrum.* **66** 716
[21] Séguin F H *et al* 2003 *Rev. Sci. Instrum.* **74** 975

[22] Li C K *et al* 2000 *Phys. Plasmas* **7** 2578
[23] Petrasso R D *et al* 2003 *Phys. Rev. Lett.* **90** 095002
[24] Delettrez J A *et al* 1987 *Phys. Rev.* A **36** 3926
[25] Oertel J A *et al* 1999 *Rev. Sci. Instrum.* **70** 803
[26] Miller J E 2004 *Bull. Am. Phys. Soc.* **49** 181
[27] Olson R E, Leeper R J, Nobile A and Oertel J A 2003 *Phys. Rev. Lett.* **91** 235002
[28] Stoeckl C *et al* 2002 *Phys. Plasmas* **9** 2195
[29] Sangster T C *et al* 2003 *Phys. Plasmas* **10** 1937
[30] Delettrez J A 2005 *et al Proc. 32nd EPS Conf. on Plasma Physics (Tarragona, Spain, 2005); Plasma Phys. Control. Fusion* **47** B791